AJR FOCUS ON:

Subarachnoid Hemorrhage: Beyond Aneurysms

Carrie P. Marder[1]
Vinod Narla
James R. Fink
Kathleen R. Tozer Fink

OBJECTIVE. Spontaneous subarachnoid hemorrhage (SAH) typically prompts a search for an underlying ruptured saccular aneurysm, which is the most common nontraumatic cause. Depending on the clinical presentation and pattern of SAH, the differential diagnosis may include a diverse group of causes other than aneurysm rupture.

CONCLUSION. For the purposes of this review, we classify SAH into three main patterns, defined by the distribution of blood on unenhanced CT: diffuse, perimesencephalic, and convexal. The epicenter of the hemorrhage further refines the differential diagnosis and guides subsequent imaging. Additionally, we review multiple clinical conditions that can simulate the appearance of SAH on CT or MRI, an imaging artifact known as pseudo-SAH.

Although trauma is the most common cause of SAH, ruptured saccular aneurysms are the most common cause of nontraumatic SAH, accounting for approximately 85% of cases of spontaneous SAH [1, 2]. Of the remaining 15% of cases, two thirds are due to idiopathic perimesencephalic hemorrhage, a benign nonaneurysmal form of SAH that is likely venous in origin [3, 4]. The remaining cases result from a wide variety of causes.

SAH can be classified into at least three distinct patterns by location on initial unenhanced CT. Recognizing these patterns facilitates the differential diagnosis and refines further imaging evaluation. Proper classification depends on unenhanced CT evaluation within 3 days of symptom onset, because substantial redistribution occurs thereafter, fundamentally altering the pattern [5]. In the first pattern, SAH is centered in the suprasellar or central basal cisterns and extends peripherally in a diffuse manner. This pattern is characteristic of saccular aneurysm rupture but may occur with other entities, such as rupture of a nonsaccular aneurysm or vascular malformation. In the second pattern, SAH is centered in the perimesencephalic or low basal cisterns and does not extend peripherally. This pattern is characteristic of idiopathic perimesencephalic hemorrhage but results from vertebrobasilar aneurysm rupture in approximately 5% of cases. Other rare causes of the perimesencephalic pattern include a cervicomedullary junction tumor, vascular malformation, or acute arterial dissection. In the third pattern, SAH is localized to the cerebral convexities alone. This pattern is infrequent, and the differential diagnosis encompasses a heterogeneous group of diseases, including reversible cerebral vasoconstriction syndrome, cerebral amyloid angiopathy (CAA), posterior reversible encephalopathy syndrome (PRES), cerebral venous thrombosis (CVT), and other less common causes. Rarely, a fourth scenario is encountered, in which no blood is visible on unenhanced CT and SAH is diagnosed by lumbar puncture.

Distinct Presentations of Subarachnoid Hemorrhage as Reflected by Anatomic Location

Suprasellar Central Cisterns With Diffuse Peripheral Extension

Characteristically, saccular aneurysms arise from branch points in the circle of Willis and produce a large volume of SAH when they rupture. Accordingly, aneurysmal SAH often fills the suprasellar, central, anterior, lateral, posterior, and lower basal cisterns and may extend to the cerebral sulci. Associated intraventricular hemorrhage sometimes occurs, such as with anterior communicating artery aneurysms that rupture into the third ventricle through the lamina terminalis. The epicenter of SAH occasionally suggests the location of an underlying ruptured saccular aneurysm. For example, SAH in the interhemispheric fissure

Keywords: convexal subarachnoid hemorrhage, perimesencephalic hemorrhage, pseudo–subarachnoid hemorrhage, subarachnoid hemorrhage

DOI:10.2214/AJR.12.9749

Received August 4, 2012; accepted after revision October 1, 2012.

[1]All authors: Department of Radiology, University of Washington, Box 357115, 1959 NE Pacific St, NW011, Seattle, WA 98195-7115. Address correspondence to C. P. Marder (cmarder@uw.edu).

This article is available for credit.

AJR 2014; 202:25–37

0361–803X/14/2021–25

suggests an anterior communicating artery aneurysm, whereas sylvian fissure SAH suggests a middle cerebral artery aneurysm. Although saccular aneurysm rupture is, by far, the most frequent nontraumatic cause of the diffuse aneurysmal pattern, trauma remains the most frequent overall cause of SAH and may produce a diffuse pattern resembling aneurysmal SAH in the setting of severe skull base fractures (Fig. 1) or acute arterial injuries. The differential diagnosis of diffuse SAH (Table 1) also includes ruptured nonsaccular aneurysm, arteriovenous malformation (AVM), or dural arteriovenous fistula (DAVF) (Fig. 2).

Perimesencephalic and Low Basal Cisterns Only

Ten percent of spontaneous SAH cases are due to benign venous bleeding known as nonaneurysmal perimesencephalic hemorrhage [3] (Fig. 3). In 1985, van Gijn et al. [3] described a series of patients with SAH and normal angiograms who had a predominance of SAH confined to the cisterns surrounding the midbrain. This pattern occurred in 13 of 28 patients with SAH and normal angiograms but in only 1 of 92 patients with SAH and ruptured aneurysms. Subsequent studies [5, 6] refined the definition of perimesencephalic hemorrhage as follows: first, blood is centered immediately anterior to the midbrain or pons and may variably involve the interpeduncular, crural, ambient, quadrigeminal, prepontine, or carotid cisterns; second, blood may thinly extend into the suprasellar cistern and the basal portions of the sylvian and interhemispheric fissures, but may not extend into the distal portions of the sylvian or interhemispheric fissures; and third, small amounts of blood may sediment in the occipital horns of the lateral ventricles, but there is no frank intraventricular hemorrhage.

These criteria apply only to unenhanced CT obtained within 3 days of symptom onset, because redistribution of SAH may considerably alter the initial pattern. In approximately 95% of cases that meet these criteria, no aneurysm is found and the clinical course is favorable, with little to no risk of rebleeding, vasospasm, or symptomatic hydrocephalus [3, 7, 8]. The presumed cause is venous rupture [3, 4]. Only 5% of cases meeting these criteria are due to ruptured vertebrobasilar aneurysms [5, 6]. Other rare causes include posterior fossa and cervical spinal AVMs, DAVFs, and vascular tumors such as hemangioblastomas (Fig. 4 and Table 1). Trauma leading to arterial dissection or venous injury at the tentorial margin may also produce this pattern.

Peripheral Convexal Subarachnoid Hemorrhage Alone

SAH may be localized to a few sulci of the cerebral convexities or to one of the sylvian fissures, without basal cistern or ventricular involvement. In the absence of trauma, isolated peripheral convexal SAH is rare. The condition may be underrecognized and has only recently been described as a distinct category of disease [9–16], with an estimated incidence of 7% of all cases of spontaneous SAH [14].

In the largest reported series of 29 patients with nontraumatic isolated convexal SAH [14], the leading diagnoses were reversible cerebral vasoconstriction syndrome (Fig. 5) and CAA (Fig. 6). Other reported causes (Table 1) include PRES (Fig. 7), CVT (Fig. 8), infectious causes (Figs. 9 and 10), coagulation disorders (Fig. 11), and moyamoya disease [9–11, 13, 14] (Fig. 12). Rare causes include ruptured superficial vascular malformations, tumors, and cerebral vasculitis [13, 17–21]. No cause is identified in 14–35% of cases [9, 11, 14]. Ruptured saccular aneurysms of the circle of Willis are not reported to cause isolated convexal SAH.

There are two main clinical presentations of convexal SAH, roughly stratified by patient age [14]. Younger patients (≤ 60 years old) are more likely to have reversible cerebral vasoconstriction syndrome and to present with sudden severe headache sometimes accompanied by neurologic deficits or stroke. Headache characteristics may be indistinguishable from those of aneurysmal SAH. Older patients (> 60 years old) are more likely to have CAA and to present with transient sensory or motor symptoms, such as numbness, tingling, or weakness. These symptoms occur with convexal SAH due to CAA, as well as other causes [22], and are probably related to cortical irritation by blood products in the subarachnoid space. Headache is another common clinical feature in this patient group, but the onset is usually more gradual and the intensity less severe compared with the "thunderclap" headache characteristic of aneurysmal SAH. Other clinical presentations of convexal SAH include altered mental status, lethargy, confusion, or seizures.

Reversible cerebral vasoconstriction syndrome—Reversible cerebral vasoconstriction syndrome is characterized clinically by the sudden onset of severe headache, sometimes accompanied by neurologic deficits, hemorrhage, or ischemia. The entity classically affects young to middle-aged women after exposure to a trigger, such as vasoactive or sympathomimetic agents, including migraine medications, stimulants such as caffeine or amphetamines, serotonergic antidepressants, and smoking tobacco or marijuana. Other triggers include strenuous activity, such as sexual intercourse or exercise, or bathing in hot or cold water.

Imaging may initially be normal or may show isolated convexal SAH (Fig. 5A), parenchymal or subdural hemorrhages, or infarcts (ischemic or hemorrhagic) [23–25]. Data from large prospective series suggest that convexal SAH is the most common early complication of reversible cerebral vasoconstriction syndrome, found in approximately 20–25% of cases [23]. The hallmark finding on vascular imaging is segmental vasoconstriction (Fig. 5B) that resolves spontaneously or with supportive treatment, including removal of triggers and short-term use of calcium channel blockers.

Cerebral amyloid angiopathy—CAA is defined histopathologically by the deposition of amyloid protein in cortical and leptomeningeal vessels. Because establishing a tissue diagnosis is invasive, the Boston criteria have been developed that allow the noninvasive designations of "possible" or "probable" CAA for patients older than 50 years who have lobar hemorrhages or cortical or subcortical microhemorrhages on imaging [26]. Convexal SAH has been increasingly recognized in association with CAA, usually in elderly patients presenting with transient ischemic attack–like symptoms [14, 16, 27–32]. Acutely, convexal SAH is best visualized on unenhanced CT or FLAIR images and may not be visible on gradient-recalled echo or susceptibility-weighted images. Gradient-recalled echo and susceptibility-weighted images are highly sensitive to detect prior episodes of convexal SAH, showing low-signal-intensity hemosiderin filling a sulcus (subarachnoid siderosis) or staining the underlying cortex (superficial cortical siderosis) [29] (Fig. 6). Accordingly, a modification to the Boston criteria has been proposed that would include these findings [30].

Posterior reversible encephalopathy syndrome—PRES is a clinical-radiologic entity most commonly associated with pregnancy-induced hypertension, eclampsia, severe hypertension of any cause, and the use of the immunosuppressive medications cyclosporine and tacrolimus after solid-organ or allogeneic

TABLE 1: Differential Diagnosis of Subarachnoid Hemorrhage by Pattern of Hemorrhage

Diffuse	Perimesencephalic	Convexal
Trauma	Trauma	Trauma
Saccular aneurysm	Nonaneurysmal perimesencephalic hemorrhage	Reversible cerebral vasoconstriction syndrome
Nonsaccular aneurysm	Saccular aneurysm	Cerebral amyloid angiopathy
Arterial dissection	Nonsaccular aneurysm	Posterior reversible encephalopathy syndrome
Vascular malformation	Arterial dissection	Cerebral venous thrombosis
Tumor	Vascular malformation (consider spinal)	Septic emboli, septic aneurysm
Vasculitis	Tumor (consider spinal)	Coagulopathy
		Moyamoya disease
		Vascular malformation (superficial)
		Tumor
		Vasculitis

bone-marrow transplantation. PRES may occur in a wide variety of other clinical conditions and is sometimes idiopathic. Other common terms referring to the same entity include "reversible posterior leukoencephalopathy" and "hypertensive encephalopathy." Patients present with seizures, headache, visual loss, or altered mental status. PRES is an important cause of isolated convexal SAH that has been recognized in multiple small series and case reports [9–11, 14, 33–35] (Fig. 7A).

Vasogenic edema involving the subcortical white matter of the parietal, occipital, or posterior frontal lobes bilaterally, and sometimes involving the cerebellum, basal ganglia, thalamus, or brainstem, is characteristic of PRES (Fig. 7B). Occasionally, PRES may manifest as restricted diffusion, enhancement, and hemorrhages, including convexal SAH, lobar hematomas, and microhemorrhages [36, 37].

Cerebral venous thrombosis—Venous thrombosis involving either a cortical vein or dural venous sinus is an important cause of convexal SAH [38–40] (Fig. 8). Patients present clinically with headache, seizures, altered mental status, and sequelae of increased intracranial pressure, such as papilledema. Hallmark findings include the cord sign (i.e., a hyperdense cortical vein on unenhanced CT) and the empty delta sign (i.e., nonfilling of the superior sagittal sinus on CT venography). Commonly described parenchymal findings result from venous hypertension and include cerebral edema, parenchymal hemorrhages, and ischemic and hemorrhagic infarcts. SAH is a relatively uncommon complication, likely resulting from rupture of thin-walled cortical veins under elevated pressure. In this setting, SAH is usually found within the cerebral convexities or sylvian fissures, sparing the basal cisterns [40].

Infectious causes—SAH complicates approximately 1–2% of cases of infectious endocarditis. The distribution of SAH is usually convexal (Fig. 9A) or localized within one sylvian fissure, but may be diffuse [41] or may be occult on CT [42]. Patients may have a history of injection drug use and present with fever, headache, mental status changes, and physical examination signs of systemic emboli. Associated imaging findings include embolic infarcts (Fig. 9B), microhemorrhages (Figs. 9C and 9D), or microabscesses. Although some cases are secondary to rupture of septic (mycotic) aneurysms (Fig. 10), angiography may be normal. In this case, SAH may result from focal endarteritis, vessel rupture at the site of embolic occlusion, or occult septic aneurysm. Brain abscesses in the early cerebritis stage may also rarely present with convexal SAH [43].

Coagulopathies—Anticoagulation and coagulation disorders such as idiopathic thrombocytopenia can also cause isolated convexal SAH [11, 14]. Complex disorders such as disseminated intravascular coagulation, usually occurring as a complication of systemic sepsis, may also lead to convexal SAH [44] (Fig. 11). SAH in this setting may result from a systemic cascade of microclot formation, consumption of platelets and clotting factors, small vessel occlusions, and bleeding manifestations.

Moyamoya disease—Moyamoya ("puff of smoke" in Japanese) refers to the distinctive angiographic appearance of collateral lenticulostriate vessels that develop after chronic stenosis of the intracranial internal carotid arteries and proximal branches of the circle of Willis. The condition may be congenital (idiopathic) or acquired after progressive vascular occlusion from any cause. Conditions associated with moyamoya disease include sickle cell disease, neurofibromatosis type 1, Down syndrome, and connective tissue diseases. Patients present with headaches, hypoperfusion symptoms, transient ischemic attacks, or strokes and may have infarcts or hemorrhages. With disease progression, transdural and transosseous pial collaterals from external carotid artery branches may develop, and these abnormal fragile collateral vessels may rupture, leading to SAH [45, 46] (Fig. 12). Saccular aneurysms may also form, so associated aneurysm rupture should be actively excluded in patients with moyamoya disease and SAH.

Special Cases

There are several rare causes of SAH that lack specific imaging features on unenhanced CT and could produce SAH in any anatomic distribution. These include both vascular and nonvascular causes. Vascular causes include vascular malformations and intracranial vasculitis. Vascular malformations, such as cavernous malformations, AVMs, and DAVFs, usually cause hemorrhage into the brain parenchyma or ventricles, but may occasionally cause isolated SAH in a pattern indistinguishable from aneurysm rupture, confined to the cerebral convexities, or within a perimesencephalic distribution. Rarely, a spinal vascular malformation causes SAH [19]. Intracranial vasculitis can be due to primary angiitis of the CNS or secondary to systemic vasculitis or connective tissue diseases, and typically presents with infarcts, parenchymal hemorrhages, nonspecific white matter lesions, or enhancing areas. SAH in a convexal or diffuse distribution is a rare presentation of intracranial vasculitis [17, 18]. Nonvascular causes include intraaxial and extraaxial tumors.

There are rare reports of meningiomas [21], infiltrating gliomas [47], and angiolipomas [20] presenting with SAH. Pituitary apoplexy is another rarely reported cause of SAH [2].

Pathologic Entities and Imaging Artifacts That Mimic Subarachnoid Hemorrhage

Several conditions can produce the false appearance of SAH on CT or MRI, known as pseudo-SAH (Table 2). The causes of pseudo-SAH include nonhemorrhagic subarachnoid space pathologic abnormalities, such as meningitis and leptomeningeal carcinomatosis, and imaging artifacts occurring in the absence of subarachnoid space abnormality.

Pathologic Abnormalities Affecting the Subarachnoid Space

Acute bacterial leptomeningitis results in disruption of the blood-brain barrier (BBB) and leakage of proteins into the CSF. In severe cases, the increase in CSF protein concentration may be sufficient to cause increased CSF attenuation on CT, giving the false appearance of SAH [48]. Elevated CSF protein concentration also decreases the T1 relaxation time of CSF and creates hyperintense CSF on FLAIR images, mimicking SAH [49, 50]. A similar increase in CSF signal intensity on FLAIR images has been described in leptomeningeal carcinomatosis [50, 51], also likely related to elevated CSF protein concentration.

Imaging Artifacts on CT

Patients with anoxic encephalopathy (Fig. 13) sometimes exhibit diffuse hyperdensity within the basal cisterns and subarachnoid spaces on CT, without SAH detected by lumbar puncture or autopsy [52, 53]. Pseudo-SAH in this situation results from a combination of diffuse cerebral edema, resulting in decreased attenuation of brain parenchyma, effacement of the subarachnoid spaces, and engorgement of venous structures on the pial surfaces. The apparent high attenuation of the subarachnoid spaces is largely perceptual, and the actual CT attenuation values within the basal cisterns measure lower than expected for blood products [53].

Spontaneous intracranial hypotension is reported to produce pseudo-SAH on CT, occurring in 10% of 40 consecutive patients in one series [54]. The characteristic CT findings include increased attenuation of the tentorium, basal cisterns, and sylvian fissures, corresponding to MRI findings of pachymeningeal tentorial enhancement and obliteration of the basal cisterns and sylvian fissures due to brain sagging. Subdural fluid collections were present in each case, and the authors speculate that two previously published reports that describe subdural hematomas as a cause of pseudo-SAH were likely unrecognized cases of spontaneous intracranial hypotension.

Iatrogenic causes of pseudo-SAH on CT include recently administered intrathecal or IV contrast material. Hyperdense subarachnoid material over the convexities resembling convexal SAH is sometimes found on unenhanced CT obtained after endovascular procedures, including aneurysm coiling (Fig. 14) and stroke intervention [55, 56]. The presumed mechanism is contrast material extravasation in areas of BBB breakdown related to hyperperfusion injury [56] or subclinical ischemia resulting from temporary vessel occlusion by microcatheters or balloon inflation [55]. Differentiating postprocedural contrast extravasation from SAH is important because it may affect patient treatment. Extravasated contrast material typically clears within several hours [56], helping to confirm the diagnosis.

Imaging Artifacts on MRI

FLAIR imaging is sensitive to both acute and subacute SAH, making it a viable alternative when CT is equivocal. Several clinical conditions, however, can mimic SAH on FLAIR imaging. Patients receiving general anesthesia for MRI may have diffuse FLAIR signal hyperintensity in the basal cisterns and cerebral sulci, a finding originally thought to be an effect of inhaled anesthetic agents, but later shown to result from the T1-shortening effects of the administration of 100% oxygen [57–59] (Fig. 15).

CSF pulsation artifact can also produce FLAIR signal hyperintensity in the ventricles or subarachnoid spaces that may mimic SAH. The artifact is caused by the inflow of nonnulled CSF in areas of high CSF flow rate, typically in the cervical or thoracic spinal canal, the third or fourth ventricles, cerebral aqueduct, and just superior to the foramen of Monro. Occasionally, CSF pulsation artifact interferes with evaluation of the basal cisterns in the posterior fossa. Cross-referencing with coronal and sagittal imaging planes or with faster sequences, such as gradient-recalled echo or true fast imaging with steady-state precession, is helpful [60].

An even more troublesome artifact relates to patient motion on single-shot fast spin-echo FLAIR images, a sequence reserved for moving patients. In this scenario, head displacement between the inversion and acquisition pulses may result in areas of nonnulled CSF in regions not associated with high CSF pulsatile flow, such as in the sulci overlying the frontal convexities [61]. The artifactual nature of the hyperintense CSF FLAIR signal may be difficult to appreciate, because the images may otherwise appear free of motion artifact. Increasing the inversion pulse section width or using a non–section-selective initial inversion pulse can help to reduce the artifact [61].

Pseudo-SAH on MRI has been increasingly reported in conditions associated with altered perfusion and BBB disruption, including acute ischemic stroke [62] and after carotid artery stenting [63] or balloon test occlusion [64]. The hyperintense acute reperfusion marker refers to hyperintense CSF signal on FLAIR imaging, found in association with compromised perfusion or hyperperfusion syndromes and caused by leakage of small amounts of gadolinium-based contrast material through a compromised BBB [65]. In one study, small quantities of gadolinium-based contrast material were isolated from the CSF of patients with hyperintense acute reperfusion marker, and phantom studies showed that the detected gadolinium-based contrast material concentrations produced enhancement on FLAIR images, whereas 10-fold higher concentrations were needed for enhancement on T1-weighted images [65]. Leakage of gadolinium-based contrast material has also been associated with pseudo-SAH on

TABLE 2: Differential Diagnosis of Pseudo–Subarachnoid Hemorrhage

Subarachnoid Space Pathology	CT Artifacts	MRI Artifacts on FLAIR
Meningitis	Anoxic encephalopathy	Supplemental oxygen
Leptomeningeal carcinomatosis	Spontaneous intracranial hypotension	CSF pulsation
	Iatrogenic	Patient motion on single-shot technique
		Gadolinium-based contrast material leak (particularly with renal failure or disrupted blood-brain barrier)

FLAIR images in patients with renal failure, in patients receiving high concentrations of gadolinium-based contrast material, and in seemingly healthy patients with intact renal function and an intact BBB [66].

Imaging Protocols

Unenhanced CT is the best initial test for patients clinically suspected to have SAH. When unenhanced CT findings are positive, or when clinical suspicion for aneurysm rupture is high, CT angiography (CTA) or digital subtraction angiography (DSA) is performed to exclude underlying saccular aneurysm. In some institutions, DSA may be repeated if findings are negative. The imaging evaluation of diffuse SAH is shown schematically in Figure 16A. Nonaneurysmal causes of SAH are also usually diagnosed by this standard workup for aneurysmal SAH, but MRI may be needed in select cases to exclude rare causes such as tumors.

Perimesencephalic Pattern of Subarachnoid Hemorrhage

Velthuis et al. [5] showed that if unenhanced CT was performed within 3 days of symptom onset and strict criteria were followed for defining a perimesencephalic distribution of blood, a high-quality CTA was sufficient to accurately identify the 5% of patients harboring a vertebrobasilar aneurysm, without the need for DSA and its inherent risks. These findings have been reproduced in several studies [12, 67–69] and are supported by a theoretic decision analytic model that concluded that, in order for DSA to be the preferred imaging strategy, the complication rate of catheter angiography would need to be less than 0.2% [70]. Nonetheless, institutional practices vary widely regarding imaging protocols for evaluating SAH, which may be partially informed by differences in image postprocessing techniques used for CTA reconstruction. The imaging evaluation of perimesencephalic hemorrhage is shown schematically in Figure 16B.

An additional issue is whether radiologists can accurately identify patients with a perimesencephalic hemorrhage pattern on unenhanced CT in whom aneurysms might be safely excluded by CTA alone. Although earlier studies [5, 6] reported excellent interobserver agreement, a recent study found only good inter- and intraobserver agreement in characterizing the perimesencephalic hemorrhage pattern [71]. The authors suggest that sufficient disagreement may exist to warrant caution in deciding to withhold angiography in these patients.

Convexal Subarachnoid Hemorrhage Alone

MRI may be an appropriate test in some patients presenting with isolated convexal SAH [10, 13], particularly to confirm a diagnosis of PRES or CAA. CVT may be seen on MRI but is typically confirmed by CT or MR venography. Peripheral SAH involving the sylvian fissures should probably be evaluated similarly to diffuse SAH, so as to exclude middle cerebral artery bifurcation aneurysms or septic aneurysms, which typically arise more distally than saccular aneurysms. Patients with signs of infection and convexal SAH on unenhanced CT may have septic emboli on MRI, but vascular imaging with CTA, MR angiography, or DSA may help exclude septic aneurysms. Most other patients with convexal SAH should undergo vascular imaging to evaluate for reversible cerebral vasoconstriction syndrome, vasculitis or other vasculopathies, small peripheral vascular malformations, or thrombosed veins [12]. Particular attention on these studies to higher order branches of the vascular tree is warranted to exclude such entities. The imaging evaluation of convexal SAH is shown schematically in Figure 16C.

No Visible Blood on CT

Patients presenting with sudden severe headache who are clinically suspected to have a saccular aneurysm but who have normal findings on unenhanced CT at the time of presentation should undergo delayed lumbar puncture to analyze for the presence of blood degradation products in the CSF [2, 72]. A delay of 12 hours from symptom onset is required to distinguish true xanthochromia from a traumatic tap. Patients in whom xanthochromia is detected should undergo CTA to evaluate for a saccular aneurysm. Just as for the perimesencephalic hemorrhage pattern, multiple studies have reported that CTA is sufficient to exclude an aneurysm in cases where no blood is visible on CT, without exposing the patient to the risks of DSA [12, 67–69]. Before the advent of high-quality CTA, it was argued that repeat DSA was not needed in these cases [3]. At many institutions, however, DSA is still performed after negative CTA on clinical grounds. The imaging evaluation of SAH with no visible blood on unenhanced CT is shown schematically in Figure 16D.

Conclusion

Saccular aneurysm rupture is the most common cause of SAH that diffusely fills the suprasellar and central basal cisterns and extends peripherally to the cerebral convexities. However, saccular aneurysm rupture is an uncommon cause of SAH confined to the perimesencephalic cisterns and is not a typical cause of SAH confined to the cerebral convexities. Accordingly, the imaging findings on initial unenhanced CT can help focus the differential diagnosis and guide the subsequent imaging evaluation.

References

1. Rinkel GJ, van Gijn J, Wijdicks EF. Subarachnoid hemorrhage without detectable aneurysm: a review of the causes. *Stroke* 1993; 24:1403–1409
2. van Gijn J, Rinkel GJE. Subarachnoid hemorrhage: diagnosis, causes and management. *Brain* 2001; 124:249–278
3. van Gijn J, van Dongen KJ, Vermeulen M, Hijdra A. Perimesencephalic hemorrhage: a nonaneurysmal and benign form of subarachnoid hemorrhage. *Neurology* 1985; 35:493–497
4. van der Schaaf IC, Velthuis BK, Gouw A, Rinkel GJE. Venous drainage in perimesencephalic hemorrhage. *Stroke* 2004; 35:1614–1618
5. Velthuis BK, Rinkel GJE, Ramos LMP, Witkamp TD, van Leeuwen MS. Perimesencephalic hemorrhage: exclusion of vertebrobasilar aneurysms with CT angiography. *Stroke* 1999; 30:1103–1109
6. Rinkel GJE, Wijdicks EFM, Vermeulen M, et al. Nonaneurysmal perimesencephalic subarachnoid hemorrhage: CT and MR patterns that differ from aneurysmal rupture. *AJNR* 1991; 12:829–834
7. Rinkel GJE, Wijdicks EFM. Outcome in patients with subarachnoid haemorrhage and negative angiography according to pattern of haemorrhage on computed tomography. *Lancet* 1991; 338:964–968
8. Herrmann LL, Zabramski JM. Nonaneurysmal subarachnoid hemorrhage: a review of clinical course and outcome in two hemorrhage patterns. *J Neurosci Nurs* 2007; 39:135–142
9. Spitzer C, Mull M, Rohde V, Kosinski CM. Nontraumatic cortical subarachnoid haemorrhage: diagnostic work-up and aetiological background. *Neuroradiology* 2005; 47:525–531
10. Patel KC, Finelli PF. Nonaneurysmal convexity subarachnoid hemorrhage. *Neurocrit Care* 2006; 4:229–233
11. Refai D, Botros JA, Strom RG, Derdeyn CP, Sharma A, Zipfel GJ. Spontaneous isolated convexity subarachnoid hemorrhage: presentation, radiological findings, differential diagnosis, and clinical course. *J Neurosurg* 2008; 109:1034–1041
12. Agid R, Andersson T, Almqvist H, et al. Negative CT angiography findings in patients with spontaneous subarachnoid hemorrhage: when is digital subtraction angiography still needed? *AJNR* 2010; 31:696–705
13. Cuvinciuc V, Viguier A, Calviere L, et al. Isolated acute nontraumatic cortical subarachnoid hemor-

rhage. *AJNR* 2010; 31:1355–1362

14. Kumar S, Goddeau RP, Selim MH, et al. Atraumatic convexal subarachnoid hemorrhage. *Neurology* 2010; 74:893–899
15. Beitzke M, Gattringer T, Enzinger C, Wagner G, Niederkorn K, Fazekas F. Clinical presentation, etiology, and long-term prognosis in patients with nontraumatic convexal subarachnoid hemorrhage. *Stroke* 2011; 42:3055–3060
16. Raposo N, Viguier A, Cuvinciuc V, et al. Cortical subarachnoid haemorrhage in the elderly: a recurrent event probably related to cerebral amyloid angiopathy. *EurJ Neurol* 2011; 18:597–603
17. Fukumoto S, Kinjo M, Hokamura K, Tanaka K. Subarachnoid hemorrhage and granulomatous angiitis of the basilar artery: demonstration of the varicella-zoster-virus in the basilar artery lesions. *Stroke* 1986; 17:1024–1028
18. Kumar R, Wijdicks EFM, Brown RD, Parisi JE, Hammond CA. Isolated angiitis of the CNS presenting as subarachnoid hemorrhage. *J Neurol Neurosurg Psychiatry* 1997; 62:649–651
19. Kim CH, Kim HJ. Cervical subarachnoid floating cavernous malformation presenting with recurrent subarachnoid hemorrhage. *J Neurol Neurosurg Psychiatry* 2002; 72:668
20. Vilela P, Saraiva P, Goulao A. Intracranial angiolipoma as cause of subarachnoid hemorrhage: case report and review of the literature. *Neuroradiology* 2005; 47:91–96
21. Rim N-J, Kim HS, Kim SYA. "Benign" sphenoid ridge meningioma manifesting as a subarachnoid hemorrhage associated with tumor invasion into the middle cerebral artery. *Korean J Radiol* 2008; 9:S10–S13
22. Field DK, Kleinig TJ. Aura attacks from acute convexity subarachnoid hemorrhage not due to cerebral amyloid angiopathy. *Cephalalgia* 2010; 31:368–371
23. Ducros A, Boukobza M, Porcher R, Sarov M, Valade D, Bousser MG. The clinical and radiologic spectrum of reversible cerebral vasoconstriction syndrome: a prospective series of 67 patients. *Brain* 2007; 130:3091–3101
24. Moustafa RR, Allen CMC, Baron JC. Call-Fleming syndrome associated with subarachnoid haemorrhage: three new cases. *J Neurol Neurosurg Psychiatry* 2008; 79:602–605
25. Marder CP, Donohue M, Weinstein J, Fink KR. Multimodal imaging of reversible cerebral vasoconstriction syndrome: a series of six cases. *AJNR* 2012; 33:1403–1410
26. Knudsen KA, Rosand J, Karluk D, Greenberg SM. Clinical diagnosis of cerebral amyloid angiopathy: validation of the Boston criteria. *Neurology* 2001; 56:537–539
27. Karabatsou K, Lecky BRJ, Rainov RG, Broome JC, White RP. Cerebral amyloid angiopathy with symptomatic or occult subarachnoid hemorrhage. *Eur Neurol* 2007; 57:103–105
28. Kleinig TJ, Kiley M, Thompson PD. Acute convexity subarachnoid haemorrhage: a cause of aura-like symptoms in the elderly. *Cephalalgia* 2008; 28:658–663
29. Linn J, Herms J, Dichgans M, et al. Subarachnoid hemosiderosis and superficial cortical hemosiderosis in cerebral amyloid angiopathy. *AJNR* 2008; 29:184–186
30. Linn J, Halpin A, Demaerel P, et al. Prevalence of superficial siderosis in patients with cerebral amyloid angiopathy. *Neurology* 2010; 74:1346–1350
31. Brunot S, Osseby GV, Rouaud O, et al. Transient ischaemic attack mimics revealing focal subarachnoid hemorrhage. *Cerebrovasc Dis* 2010; 30:597–601
32. Linn J. Central sulcus focal subarachnoid hemorrhage in the elderly: cerebral amyloid angiopathy is the most frequent cause. *AJNR* 2011; 32:E161
33. Teksam M, Casey SO, Michel E, Truwit CL. Subarachnoid hemorrhage associated with cyclosporine A neurotoxicity in a bone-marrow transplant recipient. *Neuroradiology* 2001; 43:242–245
34. Servillo G, Striano P, Striano S, et al. Posterior reversible encephalopathy syndrome (PRES) in critically ill obstetric patients. *Intensive Care Med* 2003; 29:2323–2326
35. Shah AK. Non-aneurysmal primary subarachnoid hemorrhage in pregnancy-induced hypertension and eclampsia. *Neurology* 2003; 61:117–120
36. McKinney AM, Short J, Truwit CL, et al. Posterior reversible encephalopathy syndrome: incidence of atypical regions of involvement and imaging findings. *AJR* 2007; 189:904–912
37. Hefzy HM, Bartynski WS, Boardman JF, Lacomis D. Hemorrhage in posterior reversible encephalopathy syndrome: imaging and clinical features. *AJNR* 2009; 30:1371–1379
38. Chang R, Friedman DP. Isolated cortical venous thrombosis presenting as subarachnoid hemorrhage: a report of 3 cases. *AJNR* 2004; 25:1676–1679
39. Oppenheim C, Domigo V, Gauvrit J-Y. Subarachnoid hemorrhage as the initial presentation of dural sinus thrombosis. *AJNR* 2005; 26:614–617
40. Benabu Y, Mark L, Daniel S, Glikstein R. Cerebral venous thrombosis presenting with subarachnoid hemorrhage: case report and review. *Am J Emerg Med* 2009; 27:96–106
41. Chukwudelunzu FE, Brown RD, Wijdicks EFM, Steckelberg JM. Subarachnoid haemorrhage associated with infectious endocarditis: case report and literature review. *Eur J Neurol* 2002; 9:423–427
42. Vincent FM, Zimmerman JE, Auer TC, Martin DB. Subarachnoid hemorrhage: the initial manifestation of bacterial endocarditis—report of a case with negative arteriography and computed tomography. *Neurosurgery* 1980; 7:488–490
43. Rhode V, van Oosterhout A, Mull M, Gilsbach JM. Subarachnoid haemorrhage as initial symptom of multiple brain abscesses. *Acta Neurochir (Wien)* 2000; 142:205–208
44. Schwartzman RJ, Hill JB. Neurologic complications of disseminated intravascular coagulation. *Neurology* 1982; 32:791–797
45. Marushima A, Yanaka K, Matsuki T, Kojima H, Nose T. Subarachnoid hemorrhage not due to ruptured aneurysm in moyamoya disease. *J Clin Neurosci* 2006; 13:146–149
46. Osanai T, Kuroda S, Nakayama N, Yamauchi T, Houkin K, Iwasaki Y. Moyamoya disease presenting with subarachnoid hemorrhage localized over the frontal cortex: case report. *Surg Neurol* 2008; 69:197–200
47. Hentschel S, Toyota B. Intracranial malignant glioma presenting as subarachnoid hemorrhage. *Can J Neurol Sci* 2003; 30:63–66
48. Mendelsohn DB, Moss ML, Chason DP, Muphree S, Casey S. Acute purulent leptomeningitis mimicking subarachnoid hemorrhage on CT. *J Comput Assist Tomogr* 1994; 18:126–128
49. Melhem ER, Jara H, Eustace S. Fluid-attenuated inversion recovery MR imaging: identification of protein concentration thresholds for CSF hyperintensity. *AJR* 1997; 169:859–862
50. Maeda M, Yagishita A, Yamamoto T, Sakuma H, Takeda K. Abnormal hyperintensity within the subarachnoid space evaluated by fluid-attenuated inversion-recovery MR imaging: a spectrum of central nervous system diseases. *Eur Radiol* 2003; 13:L192–L201
51. Tsuchiya K, Katase S, Yoshino A, Hachiya J. FLAIR MR imaging for diagnosing intracranial meningeal carcinomatosis. *AJR* 2001; 176:1585–1588
52. al-Yamany M, Deck J, Bernstein M. Pseudo-subarachnoid hemorrhage: a rare neuroimaging pitfall. *Can J Neurol Sci* 1999; 26:57–59
53. Given CA, Burdette JH, Elster AD, Williams DW. Pseudo-subarachnoid hemorrhage: a potential imaging pitfall associated with diffuse cerebral edema. *AJNR* 2003; 24:254–256
54. Schievink WI, Maya MM, Tourje J, Moser FG. Pseudo-subarachnoid hemorrhage: a CT finding in spontaneous intracranial hypotension. *Neurology* 2005; 65:135–137
55. Ozturk A, Saatci I, Pamuk AG, et al. Focal increased cortical density in immediate postembolization CT scans of patients with intracranial aneurysms. *AJNR* 2006; 27:1866–1875
56. Kumar G, Soni CR, Sahota PK. Transient CT hyperattenuation after Merci clot retrieval and intra-arterial thrombolysis in acute stroke mimicking subarachnoid hemorrhage. *J Vasc Interv Radiol* 2010; 21:281–284
57. Deliganis AV. Cerebrospinal fluid signal intensity increase on FLAIR MR images in patients under

general anesthesia: the role of supplemental O2. *Radiology* 2001; 218:152–156

58. Braga FT, Rocha AJ, Filho GH, Arikawa RK, Ribeiro IM, Fonseca RB. Relationship between the concentration of supplemental oxygen and signal intensity of CSF depicted by fluid-attenuated inversion recovery imaging. *AJNR* 2003; 24:1863–1868
59. Frigon C, Shaw DW, Heckbert SR, Weinberger E, Jardine D. Supplemental oxygen causes increased signal intensity in subarachnoid cerebrospinal fluid on brain FLAIR MR images obtained in children during general anesthesia. *Radiology* 2004; 233:51–55
60. Lisanti C, Carlin C, Banks K, Wang D. Normal MRI appearance and motion-related phenomena of CSF. *AJR* 2007; 188:716–725
61. Cianfoni A, Martin MGM, Du J, et al. Artifact simulating subarachnoid hemorrhage and intraventricular hemorrhage on single-shot, fast spin-echo fluid-attenuated inversion recovery images caused by head movement: a trap for the unwary. *AJNR* 2006; 27:843–849
62. Dechambre SD, Duprez T, Grandin CB, Lecouvet FE, Peeters A, Cosnard G. High signal in cerebrospinal fluid mimicking subarachnoid haemorrhage on FLAIR following acute stroke and intravenous contrast medium. *Neuroradiology* 2000; 42:608–611
63. Martin AJ, Saloner DA, Roberts TPL, et al. Carotid stent delivery in an XMR suite: immediate assessment of the physiologic impact of extracranial revascularization. *AJNR* 2005; 26:531–537
64. Michel E, Liu H, Remley KB, et al. Perfusion MR neuroimaging in patients undergoing balloon test occlusion of the internal carotid artery. *AJNR* 2001; 22:1590–1596
65. Köhrmann M, Struffert T, Frenzel T, Schwab S, Doerfler A. The hyperintense acute reperfusion marker on fluid-attenuated inversion recovery magnetic resonance imaging is caused by gadolinium in the cerebrospinal fluid. *Stroke* 2012; 43:259–261
66. Morris JM, Miller GM. Increased signal in the subarachnoid space on fluid-attenuated inversion recovery imaging associated with the clearance dynamics of gadolinium chelate: a potential diagnostic pitfall. *AJNR* 2007; 28:1964–1967
67. Kershenovich A, Rappaport ZH, Maimon S. Brain computed tomography angiographic scans as the sole diagnostic examination for excluding aneurysms in patients with perimesencephalic subarachnoid hemorrhage. *Neurosurgery* 2006; 59:798–801; discussion, 801–802
68. Westerlaan HE, Gravendeel J, Fiore D, et al. Multislice CT angiography in the selection of patients with ruptured intracranial aneurysms suitable for clipping or coiling. *Neuroradiology* 2007; 49: 997–1007
69. Kelliny M, Maeder P, Binaghi S, Levivier M, Regli L, Meuli R. Cerebral aneurysm exclusion by CT angiography based subarachnoid hemorrhage pattern: a retrospective study. *BMC Neurol* 2011; 11:8
70. Ruigrok YM, Rinkel GJE, Buskens E, Velthuis BK, van Gijn J. Perimesencephalic hemorrhage and CT angiography: a decision analysis. *Stroke* 2000; 31:2976–2983
71. Brinjikji W, Kallmes DF, White JB, Lanzino G, Morris JM, Cloft HJ. Inter- and intraobserver agreement in CT characterization of nonaneurysmal perimesencephalic subarachnoid hemorrhage. *AJNR* 2010; 31:1103–1105
72. van der Wee N, Rinkel GJE, Hasan D, van Gijn J. Detection of subarachnoid hemorrhage on early CT: is lumbar puncture still needed after a negative scan? *J Neurol Neurosurg Psychiatry* 1995; 58:357–359

Fig. 1—43-year-old man with severe trauma. Unenhanced CT shows extensive subarachnoid hemorrhage in central pattern, filling suprasellar (ss) and central cisterns, sylvian (Sy) and interhemispheric (i) fissures, and cerebral sulci, with associated hydrocephalus. Maxillofacial CT (not shown) showed fractures of sphenoid bone.

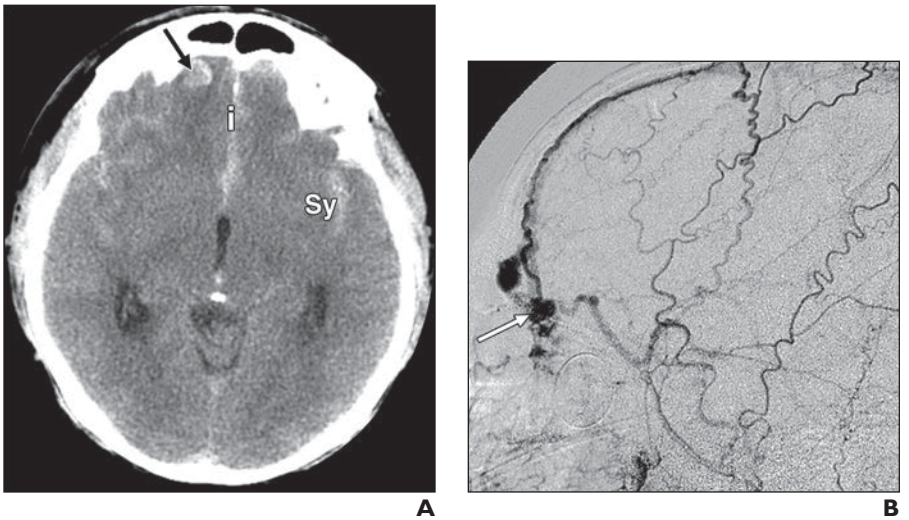

Fig. 2—51-year-old man with history of hypertension and tobacco use who awoke from sleep with worst headache of his life.
A and **B,** Unenhanced CT (**A**) shows subarachnoid hemorrhage in interhemispheric fissure (i), bilateral sylvian fissures (Sy), and bilateral cerebral convexities. Rounded density in right inferior frontal lobe (*arrow*, **A**) corresponds to dilated draining veins visible on digital subtraction angiography (DSA) (*arrow*, **B**) and CT angiography (not shown). DSA (left external carotid artery injection, lateral projection) (**B**) shows tangle of vessels near cribriform plate supplied by internal maxillary and middle meningeal arteries and drained by parasagittal cortical veins, consistent with dural arteriovenous fistula.

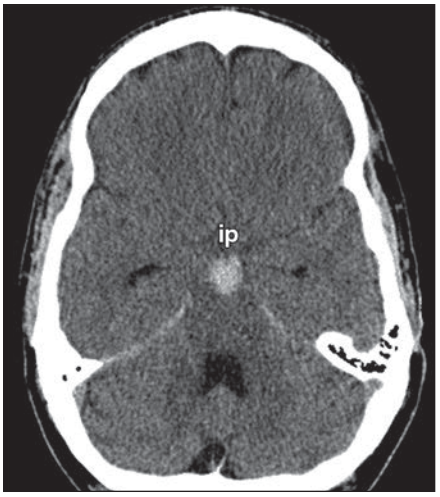

Fig. 3—58-year-old man with headache. Unenhanced CT axial image obtained on day of presentation shows subarachnoid hemorrhage concentrated in interpeduncular cistern (ip), characteristic of nonaneurysmal perimesencephalic hemorrhage. There was no extension to anterior or lateral cisterns, convexities, or ventricular system. CT angiography, digital subtraction angiography (DSA), and delayed repeat DSA (not shown) were normal with no evidence of aneurysm.

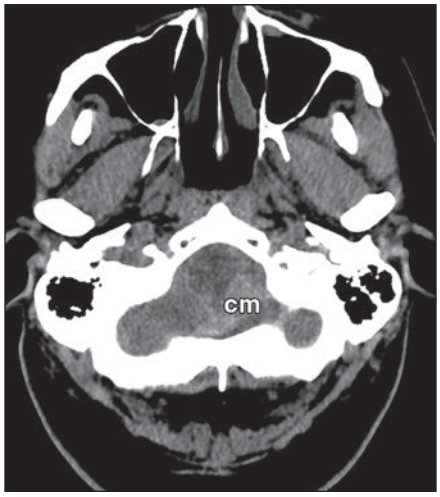

A

B

Fig. 4—55-year-old man with worst headache of his life, nausea, vomiting, and neck stiffness.
A, Unenhanced CT shows subarachnoid hemorrhage (SAH) filling cerebellomedullary cistern (cm). There was no SAH in central or suprasellar cisterns, but fourth ventricle was distended with blood (not shown), indicating cause other than benign idiopathic perimesencephalic hemorrhage.
B, Digital subtraction angiography (left vertebral artery injection, transfacial projection) shows faint abnormal blush of contrast at C1–C2 junction (*arrow*). This corresponded to homogeneously enhancing mass at cervicomedullary junction on MRI (not shown), proven to be hemangioblastoma.

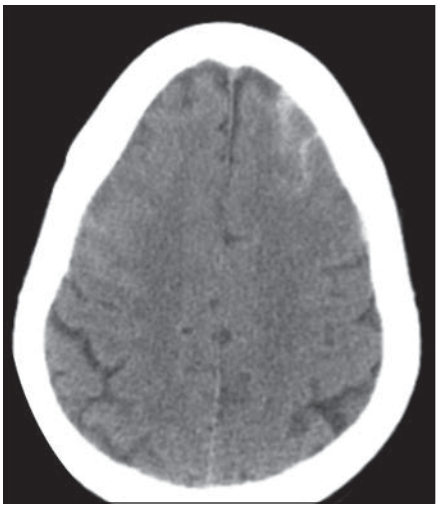

A

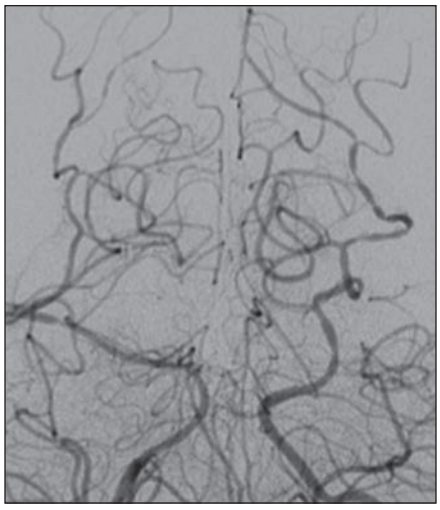

B

Fig. 5—56-year-old woman with thunderclap headache accompanied by nausea and vomiting that began while swimming in hot springs.
A, Unenhanced CT shows bilateral frontal convexal subarachnoid hemorrhage. CT angiography and digital subtraction angiography (DSA) were initially normal (data not shown), but 5 days later DSA showed diffuse segmental vasoconstriction involving multiple vascular territories.
B, DSA at day 5 (left vertebral artery injection) shows segmental vasoconstriction in posterior cerebral artery branches bilaterally, consistent with reversible cerebral vasoconstriction syndrome.

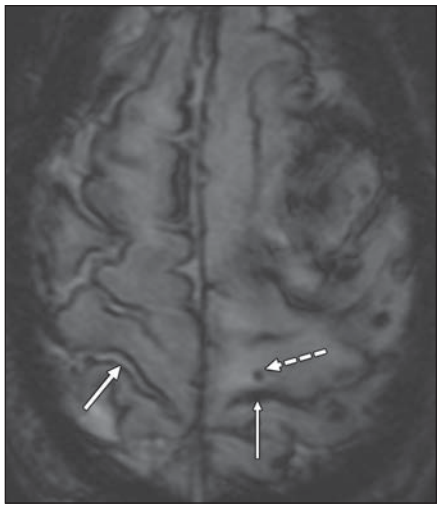

Fig. 6—60-year-old man found unconscious in his home. Gradient-recalled echo MRI shows marked diffuse cortical superficial siderosis (*thick solid arrow*), subarachnoid siderosis (*thin solid arrow*), and microhemorrhages (*dashed arrow*). Lobar hematomas were also present (not shown). Probable cerebral amyloid angiopathy with supporting pathology (from evacuated hematoma) was diagnosed using Boston criteria (see text).

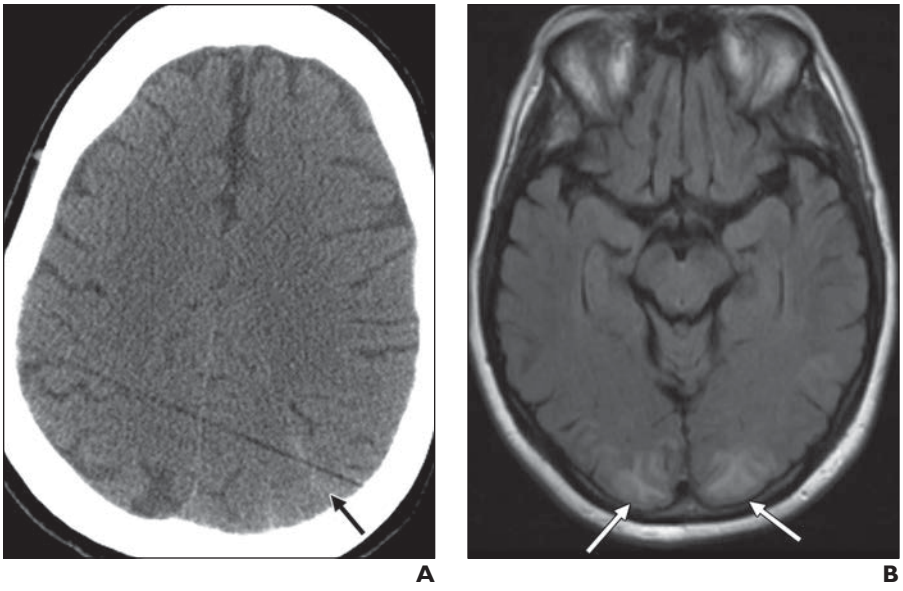

Fig. 7—69-year-old woman with history of migraine headaches who presented with severe headache for 1 day, accompanied by seizure and hypertensive emergency.
A, Unenhanced CT shows left parietal convexal subarachnoid hemorrhage (*arrow*).
B, FLAIR MRI shows bilateral occipital subcortical white matter areas of signal hyperintensity (*arrows*), consistent with posterior reversible encephalopathy syndrome. There was no associated diffusion restriction (not shown).

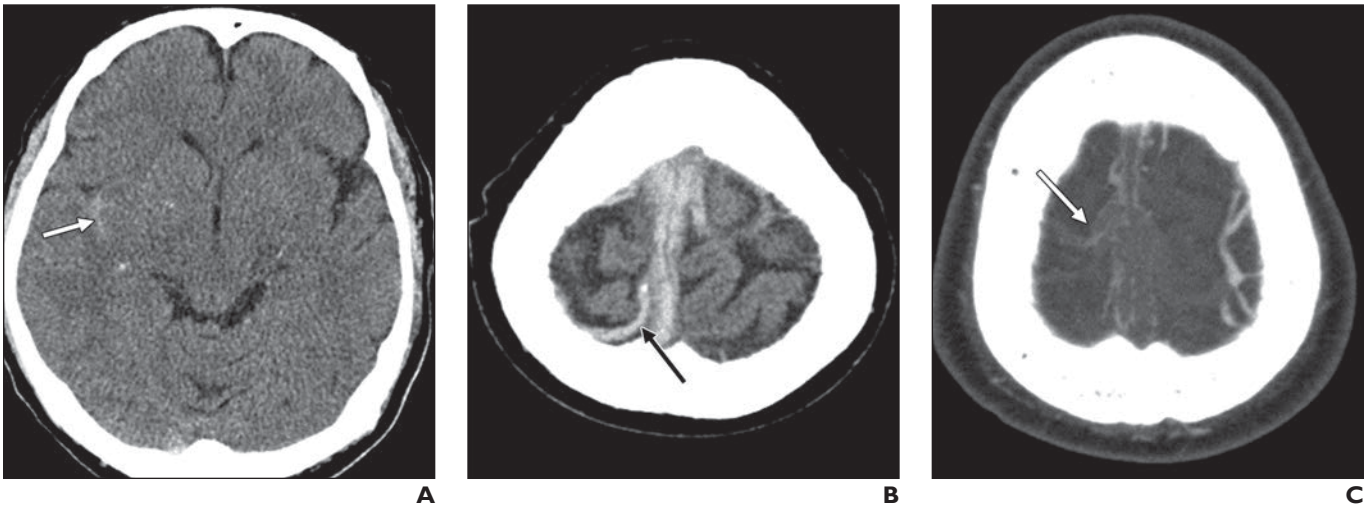

Fig. 8—68-year-old man with headache for several days and abrupt onset of left-sided weakness and seizure.
A, Unenhanced CT shows moderate subarachnoid hemorrhage filling right sylvian fissure (*arrow*) and scattered within sulci of right cerebral convexity.
B, Unenhanced CT at more superior level shows hyperdense cord sign (*arrow*).
C, CT venogram shows filling defects in corresponding right cortical veins (*arrow*) and superior sagittal sinus, consistent with cortical venous and dural sinus thrombosis.

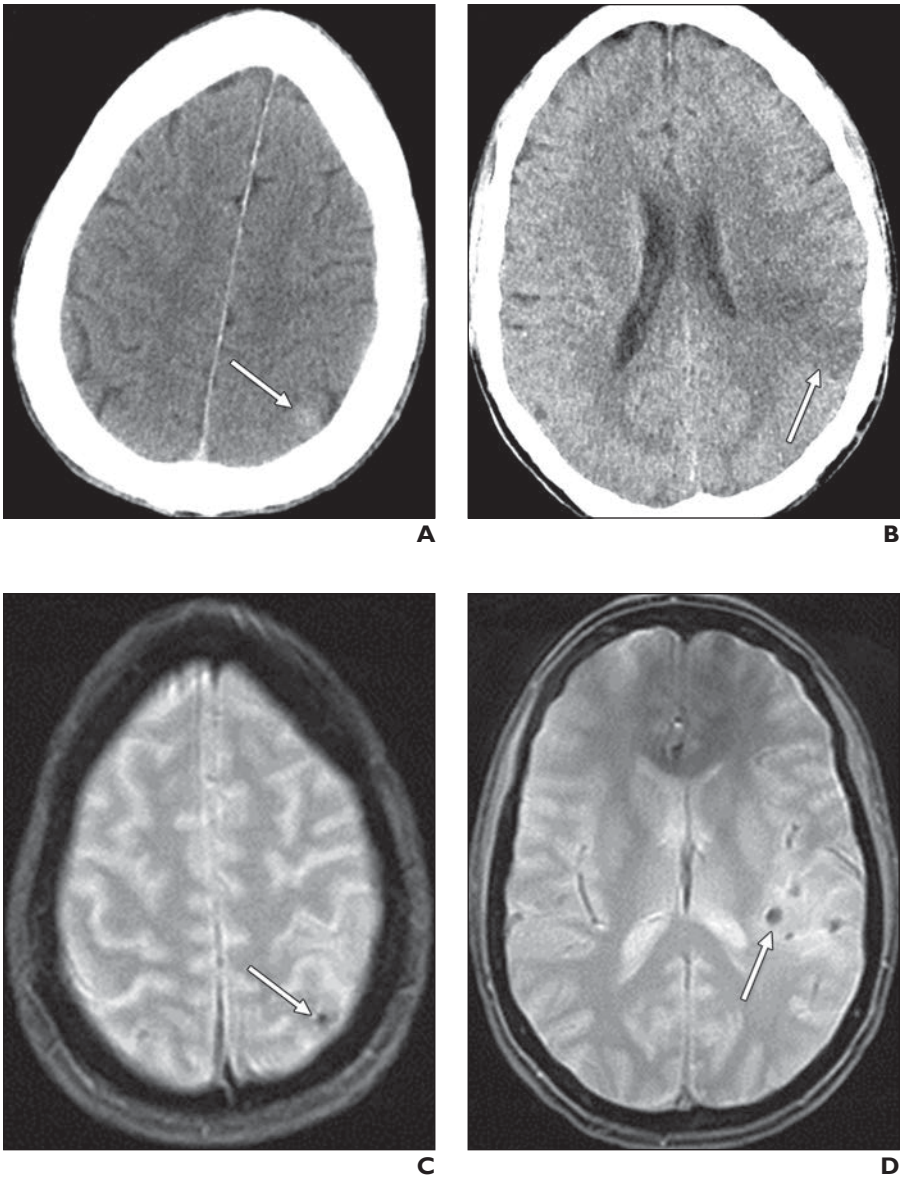

Fig. 9—44-year-old woman with history of injection drug use, now with fevers and altered mental status.
A, Unenhanced CT shows multifocal convexal subarachnoid hemorrhage (*arrow*); additional foci are not shown.
B, Four days later, she developed expressive aphasia, and repeat unenhanced CT shows new left frontoparietal acute infarct (*arrow*). Transesophageal echocardiogram revealed vegetations on mitral valve.
C and **D,** Gradient-recalled echo MRI shows foci of low signal intensity and blooming artifact (*arrows*) at locations of convexal subarachnoid hemorrhage and acute infarct, consistent with septic emboli secondary to infectious endocarditis.

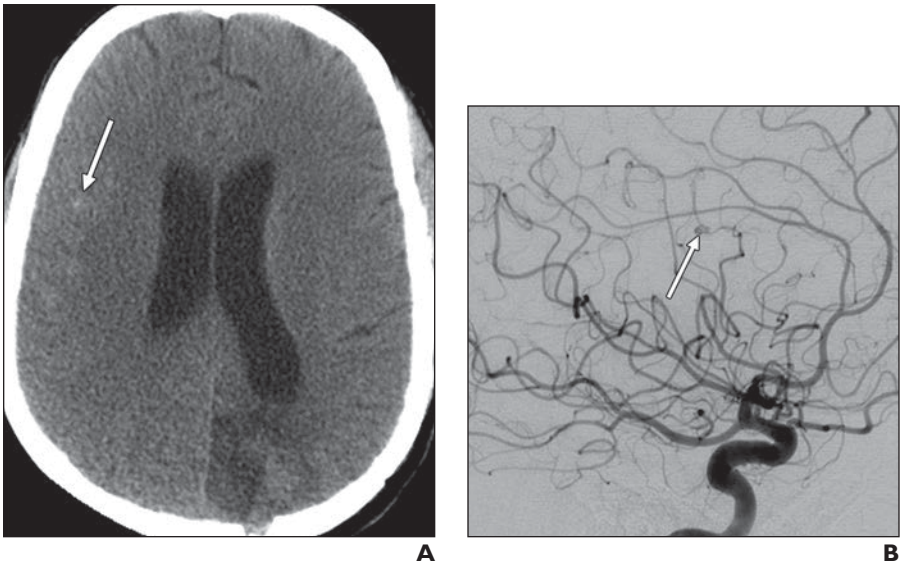

Fig. 10—54-year-old man with history of aortic valve replacement for bicuspid aortic valve, now taking warfarin (Coumadin, Bristol-Myers Squibb), who presented with worsening headache and blurry vision. One month earlier he had spontaneous intra-parenchymal hemorrhage (IPH) with negative workup.
A, Unenhanced CT shows right frontal convexal subarachnoid hemorrhage (*arrow*) and encephalomalacia at location of prior left occipital IPH.
B, CT angiography (not shown) and digital subtraction angiography, which was normal 1 month earlier (not shown), show bilobed pseudoaneurysm (*arrow*) arising from frontopolar branch of right middle cerebral artery, consistent with septic (mycotic) aneurysm.

Fig. 11—56-year-old woman with history of acute myelogenous leukemia admitted for neutropenic fever and pneumonia, now unresponsive. Unenhanced CT shows multifocal convexal subarachnoid hemorrhage (*arrow*); additional foci are not shown. Patient died soon after scan because of multiorgan failure secondary to disseminated intravascular coagulation.

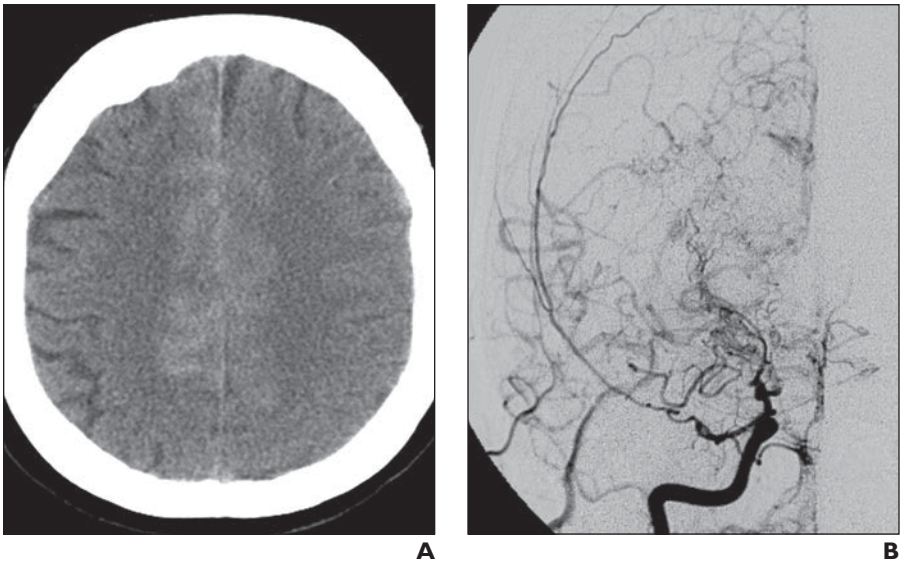

Fig. 12—35-year-old woman with severe bilateral headache and history of stroke.
A, Unenhanced CT shows convexal subarachnoid hemorrhage in parasagittal convexities bilaterally.
B, Digital subtraction angiography (right internal carotid artery [ICA] injection, anteroposterior projection) shows high-grade stenosis of right supraclinoid ICA, near-complete occlusion of M1 and A1 segments, and collateral filling of distal middle cerebral artery and anterior cerebral artery segments via pial surface collaterals and superficial temporal artery, consistent with moyamoya disease.

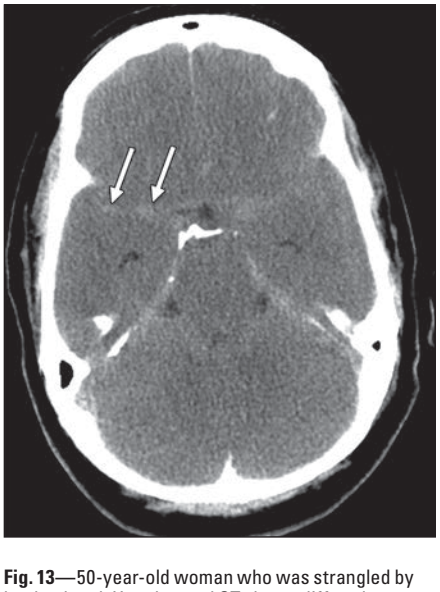

Fig. 13—50-year-old woman who was strangled by her husband. Unenhanced CT shows diffuse low attenuation with loss of gray-white differentiation, effacement of cerebral sulci, and hyperdense appearance of subarachnoid spaces (*arrows*), consistent with pseudo–subarachnoid hemorrhage due to anoxic encephalopathy. Diagnosis was supported by focal lenticular low attenuation in basal ganglia bilaterally (not shown).

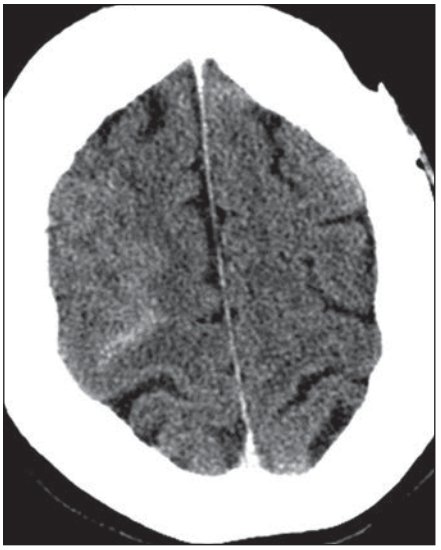

Fig. 14—70-year-old woman immediately after stenting and occlusion of right internal carotid artery aneurysm. Unenhanced CT obtained routinely shows hyperdensity in subarachnoid space overlying right frontal convexity, with associated sulcal effacement. Patient complained only of transient finger numbness. These findings persisted at 4 hours but resolved completely at 24 hours (not shown) and likely represent extravasated iodinated contrast material.

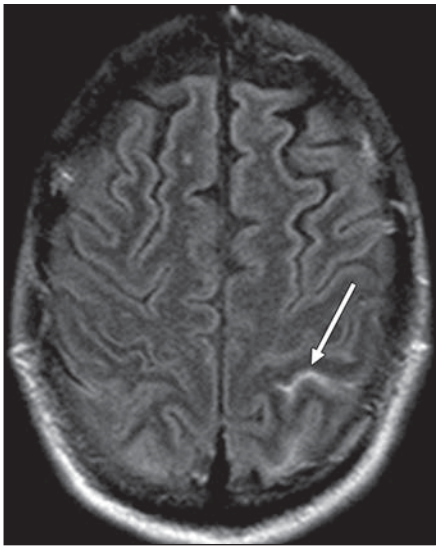

Fig. 15—58-year-old man with history of lung cancer and new-onset lower extremity weakness. FLAIR MRI shows sulcal areas of signal hyperintensity in parietal and occipital lobes, more on left side (*arrow*). Corresponding areas on unenhanced CT same day (not shown) revealed no subarachnoid hemorrhage (SAH). Findings on MRI were attributed to high-flow oxygen therapy mimicking SAH.

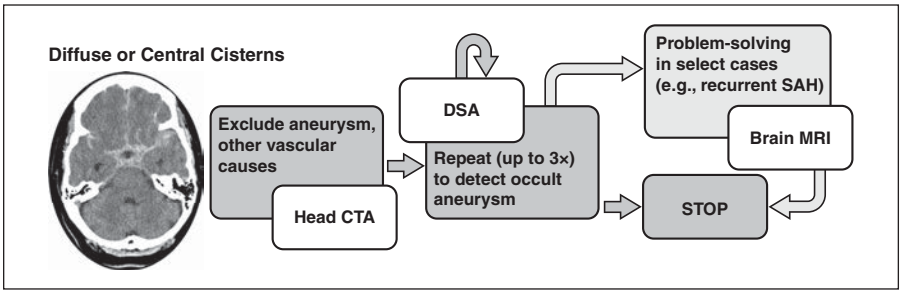

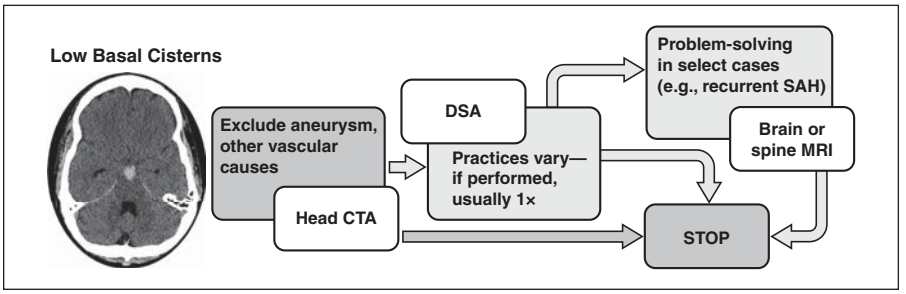

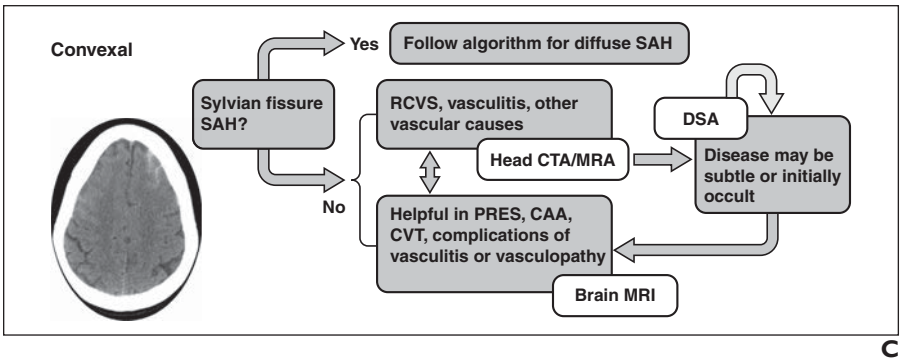

Fig. 16—Imaging approach to nontraumatic subarachnoid hemorrhage (SAH) by pattern of hemorrhage on unenhanced CT.
A–D, Schematic diagrams illustrate stepwise approach to diagnostic testing. Arrows denote transitions to next imaging steps after negative test. Dark gray boxes indicate standard steps, whereas light gray boxes indicate optional steps. Diffuse or central cistern pattern (**A**) is classic for aneurysmal SAH, and workup is directed at excluding saccular aneurysm rupture. Algorithm for low basal cisterns (**B**) applies to cases in which strict criteria for perimesencephalic hemorrhage have been met (see text). Otherwise, algorithm for diffuse SAH applies. With convexal SAH (**C**), compared with other patterns, brain MRI has more fundamental role and may be performed as initial test. CAA = cerebral amyloid angiopathy, CTA = CT angiography, CVT = cerebral venous thrombosis, DSA = digital subtraction angiography, MRA = MR angiography, PRES = posterior reversible encephalopathy syndrome, RCVS = reversible cerebral vasoconstriction syndrome.

(Fig. 16 continues on next page)

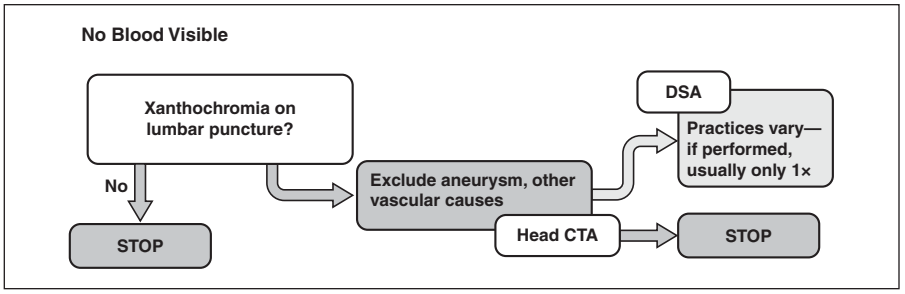

D

Fig. 16 (continued)—Imaging approach to nontraumatic subarachnoid hemorrhage (SAH) by pattern of hemorrhage on unenhanced CT. **A–D,** In cases of no visible blood (**D**), vascular imaging is performed only if xanthochromia is found on delayed lumbar puncture. CAA = cerebral amyloid angiopathy, CTA = CT angiography, CVT = cerebral venous thrombosis, DSA = digital subtraction angiography, MRA = MR angiography, PRES = posterior reversible encephalopathy syndrome, RCVS = reversible cerebral vasoconstriction syndrome.

FOR YOUR INFORMATION

This article is available for CME and Self-Assessment (SA-CME) credit that satisfies Part II requirements for maintenance of certification (MOC). To access the examination for this article, follow the prompts associated with the online version of the article.